On the Galilean invariance of some dispersive wave equations

Angel Duran, Denys Dutykh, Dimitrios Mitsotakis

ON THE GALILEAN INVARIANCE OF SOME DISPERSIVE WAVE EQUATIONS

ANGEL DURAN, DENYS DUTYKH*, AND DIMITRIOS MITSOTAKIS

Abstract. Surface water waves in ideal fluids have been typically modeled by asymptotic approximations of the full Euler equations. Some of these simplified models lose relevant properties of the full water wave problem. One of them is the Galilean symmetry, which is not present in important models such as the BBM equation and the Peregrine (Classical Boussinesq) system. In this paper we propose a mechanism to modify the above mentioned classical models and derive new, Galilean invariant models. We present some properties of the new equations, with special emphasis on the computation and interaction of their solitary-wave solutions. The comparison with full Euler solutions shows the relevance of the preservation of Galilean invariance for the description of water waves.

Contents

1. Introduction 2
2. Mathematical models 3
2.1. The KdV equation 4
2.2. The BBM equation 5
2.3. The iBBM equation 6
2.4. The Peregrine system 8
2.5. The iPeregrine system 9
2.6. The Serre equations 10
3. Numerical computation of travelling waves 10
3.1. Computation of travelling-wave profiles. The Petviashvili method 11
3.2. Tanaka's solution 13
3.3. Fenton's asymptotic solution 15
3.4. Numerical results 15
4. Solitary waves interactions 18
4.1. Head-on collisions of solitary waves 21
4.2. Overtaking interactions of solitary waves 22
4.3. Comparison with Euler equations 24
5. Conclusions 25
Acknowledgements 28
References 28

Key words and phrases. water waves; Galilean invariance; Boussinesq equations; Peregrine system; BBM equation; dispersive waves; solitary waves.

* Corresponding author.

1. Introduction

The purpose of this paper is to investigate the relevance of the Galilean invariance in the description of water waves. Some classical approximate models are reviewed. Those without the property of invariance under Galilean transformations are modified and the corresponding invariant versions are formulated. The new models are considered as approximations to the full Euler equations and compared with the classical systems. The comparison is focused on the existence and the dynamics of solitary waves.

A natural argument in mathematical modeling is the inheritance of the physical properties of the phenomenon under study through the introduction of mathematical devices. In the case of water wave theory, the approximation to the full Euler equations leads to some mathematical models in which some fundamental properties of the original problem can be lost. This is relevant in the case of symmetries. For example, when asymptotic expansions around the still water level are performed, the invariance under vertical translations can be broken and the derived model is valid only in this particular frame of reference. Dispersive wave models possessing the property of invariance under vertical translations have been shown to be particularly robust for the simulation of the long wave runup, cf. [31]. A second symmetry, which this paper is focused on, is related to the universality of mechanical laws in all inertial frames of reference. The Galilean invariance (or Galilean relativity) is one of the fundamental properties of any mathematical model arising in classical mechanics. This principle was empirically established by Galileo Galilei 55 years before the formulation of Newton's laws of mechanics in 1687, [57]. Nowadays, it is common to speak about this principle in terms of a symmetry of the governing equations, [59]. For instance, the complete water wave problem possesses naturally this property. (For a systematic study of symmetries and conservation laws of the full water wave formulation we refer to Benjamin & Olver (1982), [5]). Nevertheless, numerous dispersive wave equations, some of them being well-known, are not invariant under the Galilean transformation. This issue was already addressed in a previous study by Christov (2001), [19]. We note that some fully nonlinear approximations such as Nonlinear Shallow Water Equations (NSWE), [24, 6, 41, 54, 33, 32], improved Shallow Water Equations, [29], and the Serre or Green-Naghdi equations, [68, 37, 38, 42, 26, 17, 20], are invariant under the vertical translation and the Galilean boost. Some other examples of some Boussinesq-type systems which are not Galilean invariant can be found in [12, 58, 7, 8]. It is finally noted that the idea of exploiting symmetries of continuous equations has already been shown very beneficial in improving the behavior of underlying numerical discretizations, [43, 44, 18].

However, to our knowledge, the practical implications of the loss of the Galilean symmetry are not sufficiently known. In the present study we try to shed some light on this issue and its influence on the approximate dispersive wave models.

The paper is organized as follows. In Section 2 we review some classical models in water wave theory and present the invariant counterparts of the BBM equation and the classical Peregrine system. A way to asses the accuracy of the invariantized models is by comparing their travelling wave solutions to the corresponding ones of the full Euler equations and of

the rest of the classical models under consideration. In Section 3, solitary-wave profiles of the new models are generated numerically. The comparison with the wave profiles of other approximations (some with exact formulas) and of the Euler equations (by using Tanaka's algorithm and Fenton's asymptotic solution) is established in terms of the amplitude-speed and amplitude-shape relations. The interactions of solitary waves for the new models, with head-on and overtaking collisions, are studied in Section 4. Finally, the main conclusions of this study are outlined in Section 5.

2. Mathematical models

Consider an ideal fluid of constant density along with a cartesian coordinate system in two space dimensions (x, y). The y-axis is taken vertically upwards and the x-axis is horizontal and coincides traditionally with the still water level. The fluid is bounded below by an impermeable horizontal bottom at $y = -d$ and above by an impermeable free surface at $y = \eta(x, t)$. We assume that the total depth $h(x, t) \equiv d+\eta(x, t)$ remains positive $h(x, t) \geqslant h_0 > 0$ at all times t. The sketch of the physical domain is shown in Figure 1.

Assuming that the flow is incompressible and irrotational, the governing equations of the classical water wave problem are the following, [47, 69, 55, 72]

$$\phi_{xx}^2 + \phi_{yy}^2 = 0 \qquad -d \leqslant y \leqslant \eta(x,t), \tag{2.1}$$

$$\eta_t + \phi_x\,\eta_x - \phi_y = 0 \qquad y = \eta(x,t), \tag{2.2}$$

$$\phi_t + \tfrac{1}{2}\,(\phi_x)^2 + \tfrac{1}{2}\,(\phi_y)^2 + g\,\eta = 0 \qquad y = \eta(x,t), \tag{2.3}$$

$$\phi_y = 0 \qquad y = -d, \tag{2.4}$$

with ϕ being the velocity potential (by definition, the irrotational velocity field $u = \phi_x$ and g the acceleration due to the gravity force. The water wave problem possesses Hamiltonian, [65, 75, 14, 67], and Lagrangian, [53, 20], variational structures.

Remark 1. *We make the classical assumption that the free surface is a graph $y = \eta(x, t)$ of a single-valued function. This means in practice that we exclude some interesting phenomena, (e.g., wave breaking) which are out of the scope of this modeling paradigm.*

Remark 2. *We underline the fact that in the presence of a free surface the vorticity does not remain zero even if it is so initially. Any singularity at the free surface may lead the vortex sheets creation. However, the water wave theory is not supposed to hold when a wave breaking event occurs.*

The symmetry group of the complete water wave problem (2.1) – (2.4) was described by Benjamin & Olver (1982) in [5]. In particular, the full formulation of the water wave equations admits the Galilean boost symmetry and the invariance under the vertical translations (the latter issue will be addressed by the authors in a future work). However, the water wave theory has been developed from the beginning by constructing various approximate models which may conserve or break some of the symmetries, [23]. Below we consider several classical models and discuss their Galilean invariance property.

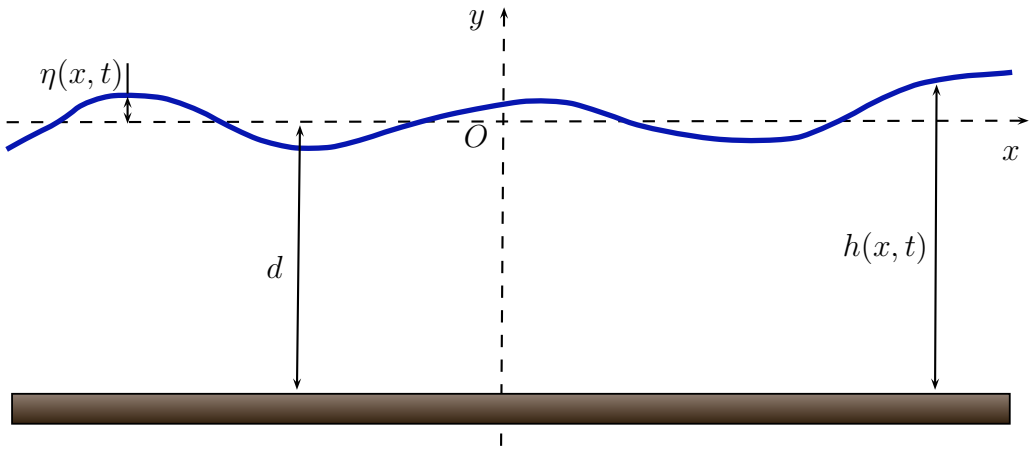

FIGURE 1. Sketch of the physical domain.

2.1. **The KdV equation.** The unidirectional propagation of long waves in the so-called Boussinesq regime (where the nonlinearity and the dispersion are of the same order of magnitude), [13, 8, 30], can be described by the celebrated Korteweg–de Vries (KdV) equation [45, 40], which in dimensional variables is written in the form:

$$u_t + \sqrt{gd}\, u_x + \frac{3}{2} u u_x + \frac{d^2}{6}\sqrt{gd}\, u_{xxx} = 0, \tag{2.5}$$

where $u(x,t)$ is the horizontal velocity variable which is usually defined as the depth-averaged velocity, [64], or the fluid velocity measured at some specific water depth, [12, 58]. Some very well-known properties of (2.5) are reviewer (see e.g. [36, 48, 56]). First, the KdV equation is an integrable model with the following two-parameter family of solitary wave solutions:

$$u(x,t) = u_0 \operatorname{sech}^2\big(\tfrac{1}{2}\kappa(x - c_s t - x_0)\big), \quad c_s = \sqrt{gd} + \frac{u_0}{2}, \quad (\kappa d)^2 = \frac{3u_0}{\sqrt{gd}}, \quad u_0 > 0, x_0 \in \mathbb{R}.$$

The initial value problem of the Korteweg–de Vries (KdV) equation possesses a Hamiltonian structure

$$u_t = \mathbb{J}\frac{\delta \mathcal{H}}{\delta u},$$

(where δ denotes the variational derivative) in a suitable phase space of functions vanishing, along with some of their derivatives, at infinity. The skew-symmetric operator $\mathbb{J}$ and the Hamiltonian functional $\mathcal{H}$ are

$$\mathbb{J} = -\partial_x, \qquad \mathcal{H} = \frac{1}{2}\int_{\mathbb{R}} \Big[\sqrt{gd}u^2 + \tfrac{1}{2}u^3 - \sqrt{gd}\,\frac{d^2}{6}u_x^2\Big]\mathrm{d}x.$$

The Hamiltonian $\mathcal{H}$ is the third conserved quantity of the well-known hierarchy of invariants for (2.5), [48].

The central question in our study is the Galilean invariance of model equations. We can show that the KdV equation (2.5) possesses this property. The procedure is as follows. We choose another frame of reference which moves uniformly, for example, rightwards

with constant celerity c. This symmetry is expressed by the following transformation of variables:

$$x \to x - \tfrac{3}{2}ct, \quad t \to t, \quad u \to u + c. \tag{2.6}$$

In this moving frame of reference (2.5) becomes:

$$u_t - \frac{3}{2}cu_x + \sqrt{gd}\,u_x + \frac{3}{2}(u+c)u_x + \frac{d^2}{6}\sqrt{gd}\,u_{xxx} = 0.$$

After some simplifications one can recover the original KdV equation, which completes the proof of the invariance.

In order to assess the relative magnitude of various terms in equation (2.5) scaled variables are introduced. The classical long wave scaling is the following:

$$x' := \frac{x}{\ell}, \quad y' := \frac{y}{d}, \quad t' := \frac{g}{d}t, \quad \eta' := \frac{\eta}{a}, \quad u' := \frac{u}{\sqrt{gd}}, \tag{2.7}$$

where h_0, a, ℓ are the characteristic water depth, wave amplitude and wave length respectively. Using these three characteristic lengths we can form three following important dimensionless numbers:

$$\varepsilon := \frac{a}{d}, \quad \mu^2 := \left(\frac{d}{\ell}\right)^2, \quad \mathrm{S} := \frac{\varepsilon}{\mu^2}. \tag{2.8}$$

Parameters $\varepsilon \ll 1$ and $\mu^2 \ll 1$ characterize the wave nonlinearity and dispersion, while the so-called Stokes number S measures the analogy between these two effects. In the Boussinesq regime the Stokes number is of order of one, $\mathrm{S} = \mathcal{O}(1)$, which establishes that the dispersion and the nonlinear effects are comparable. The relevance of this parameter is discussed by Ursell (1953), cf. e.g. [71].

Using these dimensionless and scaled variables the KdV equation (2.5) can be written in the form:

$$u_t + u_x + \frac{3}{2}\varepsilon u u_x + \frac{\mu^2}{6}u_{xxx} = 0.$$

where the primes have been dropped. Formulas (2.7) and (2.8) will also be used in some of the developments below.

2.2. **The BBM equation.** Benjamin, Bona & Mahony (1970), [4], (see also [63]) proposed the following modification of the KdV equation, known as the BBM equation:

$$u_t + \sqrt{gd}\,u_x + \frac{3}{2}uu_x - \frac{d^2}{6}u_{xxt} = 0. \tag{2.9}$$

The main idea for the derivation of this model is to use the lower order relation between time and space derivatives in order to modify the higher-order dispersive term:

$$u_t = -u_x + \mathcal{O}(\varepsilon + \mu^2) \quad \Longrightarrow \quad u_{xxx} = -u_{xxt} + \mathcal{O}(\varepsilon + \mu^2).$$

One of the main practical motivations for this modification is to improve the dispersion relation properties of the KdV equation. Specifically, unlike the KdV equation, the phase

and group velocities of the BBM equation have a lower bound. It is also noted that the BBM equation has the following solitary wave solutions:

$$u(x,t) = u_0 \operatorname{sech}^2\big(\tfrac{1}{2}\kappa(x - c_s t - x_0)\big), \quad c_s = \sqrt{gd} + \frac{u_0}{2}, \quad (\kappa d)^2 = \frac{3u_0}{\sqrt{gd} + \frac{1}{2}u_0}, \quad x_0 \in \mathbb{R}.$$

The BBM equation is not integrable, but it can also be written as an infinite-dimensional Hamiltonian system

$$u_t = \mathbb{J}\frac{\delta \mathcal{H}}{\delta u},$$

where the operator $\mathbb{J}$ and the Hamiltonian functional $\mathcal{H}$ are defined as:

$$\mathbb{J} = (1 - \frac{d^2}{6}\partial_{xx})^{-1} \cdot (-\partial_x), \qquad \mathcal{H} = \frac{1}{2}\int_{\mathbb{R}} \big[\sqrt{gd}u^2 + \tfrac{1}{2}u^3\big]\,\mathrm{d}x. \tag{2.10}$$

and the structure is defined on a phase space similar to that of the KdV equation.

As far as the Galilean invariance is concerned, the change of variables (2.6) applied to (2.9) leads to

$$u_t - \frac{3}{2}cu_x + \sqrt{gd}\,u_x + \frac{3}{2}(u+c)u_x - \frac{d^2}{6}u_{xxt} + \frac{d^2}{4}cu_{xxx} = 0,$$

and after some algebraic simplifications we obtain:

$$u_t + \sqrt{gd}\,u_x + \frac{3}{2}uu_x - \frac{d^2}{6}u_{xxt} + \frac{d^2}{4}cu_{xxx} = 0.$$

Since there is at least one new term ($\frac{d^2}{4}cu_{xxx}$) appeared in the previous moving frame of reference, the BBM equation is not Galilean invariant. The relevance of this drawback always puzzled the researchers, cf. [19].

2.3. **The iBBM equation.** We now propose a modification to the classical BBM equation which allows us to recover the Galilean invariance property. Furthermore, the idea behind the arguments below can be extrapolated to other models. The strategy is to add a new term which will vanish the non-invariant contribution of the BBM dispersion u_{xxt} under the transformation (2.6). The resulting equation, which will be called invariant Benjamin–Bona–Mahony (iBBM) equation, takes the form:

$$u_t + \sqrt{gd}\,u_x + \frac{3}{2}uu_x - \frac{d^2}{6}u_{xxt} - \frac{d^2}{4}uu_{xxx} = 0. \tag{2.11}$$

It is straightforward to see that (2.11) is invariant under the Galilean transformation (2.6)

The modification proposed above becomes more transparent in scaled variables. The application of the long wave limit (2.7) to (2.11) leads to

$$u_t + u_x + \frac{3}{2}\varepsilon uu_x - \frac{\mu^2}{6}u_{xxt} - \frac{\varepsilon\mu^2}{4}uu_{xxx} = 0.$$

One can observe that the last term on the left hand side, responsible of the Galilean invariance of (2.11), is a nonlinear term of order $\mathcal{O}(\varepsilon\mu^2)$ and consequently, it is asymptotically negligible in the BBM formulation. Since this additional term is nonlinear, the linear

dispersion relation of (2.9) is not modified. Its effect will be studied thoroughly in the following sections.

Remark 3. *Unlike the BBM equation (2.9), this invariant version (2.11) does not possess, to our knowledge, a Hamiltonian structure. However, it is possible to propose an invariantization which preserves this variational formulation along with the Galilean invariance. The alternative given by the equation*

$$u_t + \sqrt{gd}\,u_x + \frac{3}{2}uu_x - \frac{d^2}{6}u_{xxt} - \frac{d^2}{4}\big(2u_xu_{xx} + uu_{xxx}\big) = 0. \tag{2.12}$$

has an additional higher-order nonlinear term which allows for a non-canonical Hamiltonian structure. In this case, the operator $\mathbb{J} = (1 - \frac{d^2}{6}\partial_{xx})^{-1} \cdot (-\partial_x)$ *is the same as for the BBM equation and the Hamiltonian* $\mathcal{H}$ *is*

$$\mathcal{H} = \frac{1}{2}\int_{\mathbb{R}}\Big[\sqrt{gd}u^2 + \frac{1}{2}u^3 + \frac{d^2}{4}uu_x^2\Big]\,\mathrm{d}x.$$

We underline some similarity between equation (2.12) and several proposed earlier moodels such as the Camassa-Holm [15], Burgers-Poisson [35] and Degasperis-Procesi [25] equations.

We now look for travelling wave solutions of (2.11) of the form:

$$u(x,t) = u(\xi), \qquad \xi := x - c_st, \tag{2.13}$$

where c_s is the solitary wave speed. We also assume that $u(\xi)$ decays to zero along with all derivatives when $|\xi| \to \infty$. Substituting (2.13) into the iBBM equation (2.11) leads to the ordinary differential equation:

$$(\sqrt{gd} - c_s)u' + \frac{3}{4}(u^2)' + c_s\frac{d^2}{6}u''' - \frac{d^2}{4}uu''' = 0, \tag{2.14}$$

where the prime denotes differentiation with respect to ξ. Using the boundary conditions at the infinity, the identity $uu''' = (uu'' - \frac{1}{2}(u')^2)'$, and after one integration, equation (2.14) becomes:

$$(\sqrt{gd} - c_s)u + \frac{3}{4}u^2 + c_s\frac{d^2}{6}u'' - \frac{d^2}{6}\Big(\frac{1}{2}(u')^2 - uu''\Big) = 0, \tag{2.15}$$

that can be written as a system

$$u' = v, \tag{2.16}$$

$$v' = \frac{2}{d^2\left(\frac{c_s}{3} - \frac{u}{2}\right)}\left((c_s - \sqrt{gd})u - \frac{3}{4}u^2 - \frac{d^2}{8}v^2\right). \tag{2.17}$$

Now it can be checked that when $c_s > \sqrt{gd}$, the origin $u = v = 0$ is a saddle point, as depicted in Figure 2(a), which shows the corresponding phase plane. The homoclinic trajectory $O \to A \to B \to O$ represents a solitary wave. (The MATLAB code for this figure can be found in [60].).

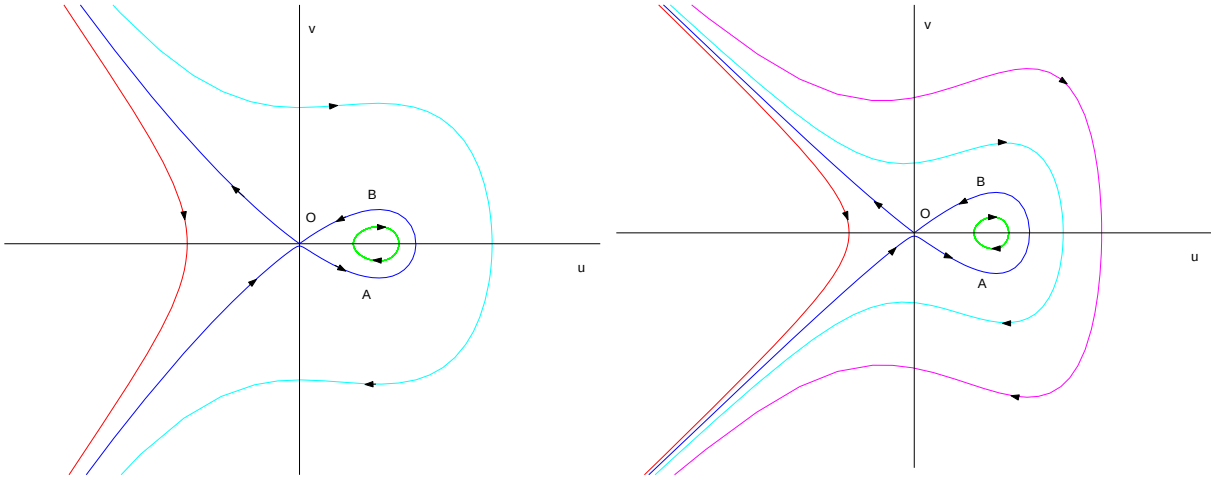

(a) (b)

FIGURE 2. Phase plane of the invariant models with $c_s > \sqrt{gd}$: (a) (iBBM). (b) (iPer). In both cases, the trajectory $O \to A \to B \to O$ represents a solitary wave.

2.4. **The Peregrine system.** Under the assumptions described above, D.H. Peregrine in 1967 derived the following system of equations governing the two-way propagation of long waves of small amplitude in the Boussinesq regime [64]:

$$\eta_t + \big((d+\eta)u\big)_x = 0, \tag{2.18}$$

$$u_t + uu_x + g\eta_x - \frac{d^2}{3}u_{xxt} = 0, \tag{2.19}$$

where $u(x,t)$ is now defined as the depth averaged fluid velocity, $\eta(x,t)$ is the deviation of the free surface of the water from its rest position. This system is also known as the Classical Boussinesq system, cf. [8] and will be denoted by (cPer). In [61], the existence and some properties of solitary wave solutions of (2.18)-(2.19) are obtained, without explicit formulas. On the other hand, to our knowledge, a Hamiltonian structure has not been found, [8].

We now study the Galilean invariance of (2.18)-(2.19). In this case, the Galilean transformation takes the following form:

$$x \to x - ct, \quad t \to t, \quad \eta \to \eta, \quad u \to u + c. \tag{2.20}$$

The mass conservation equation (2.18) in new variables reads:

$$\eta_t - c\eta_x + \big((d+\eta)(u+c)\big)_x = 0.$$

After simplifications one can see that this equation remains invariant under the transformation (2.20).

Now let us consider the momentum balance equation (2.19). In the moving frame of reference this equation becomes:

$$u_t - cu_x + (u+c)u_x + g\eta_x - \frac{d^2}{3}u_{xxt} + c\frac{d^2}{3}u_{xxx} = 0,$$

and after some manipulations

$$u_t + uu_x + g\eta_x - \frac{d^2}{3}u_{xxt} + c\frac{d^2}{3}u_{xxx} = 0.$$

As in the BBM case, a new dispersive term $c\frac{d^2}{3}u_{xxx}$ appears, showing that the system (2.18)-(2.19) is not Galilean invariant.

2.5. **The iPeregrine system.** Following the same technique as in the case of the BBM equation, it is possible to propose a modification to the classical Peregrine system (2.18)-(2.19) which will allow us to recover the Galilean invariance property. It can be done in a way leading to the iBBM equation (2.11). The corresponding system reads:

$$\eta_t + \big((d+\eta)u\big)_x = 0, \tag{2.21}$$

$$u_t + uu_x + g\eta_x - \frac{d^2}{3}u_{xxt} - \frac{d^2}{3}uu_{xxx} = 0. \tag{2.22}$$

Note that since the mass conservation equation is invariant, it is not modified in the new version. Now it is straightforward to check the invariance of equation (2.22). Therefore, system (2.21)-(2.22), which will be called invariant Peregrine system or (iPer) for the sake of conciseness, is Galilean invariant. In dimensionless and scaled variables, the system reads:

$$\begin{aligned} \eta_t + \big((1+\varepsilon\eta)u\big)_x &= 0, \\ u_t + \varepsilon uu_x + \eta_x - \frac{\mu^2}{3}u_{xxt} - \frac{\varepsilon\mu^2}{3}uu_{xxx} &= 0, \end{aligned}$$

and one can see that the new term is of higher-order and, asymptotically speaking, negligible. As in the case of the Peregrine system, equations (2.21)-(2.22) do not possess, to our knowledge, a Hamiltonian structure.

Finally, we can look for travelling wave solutions of system (2.21)-(2.22) of the form

$$\eta(x,t) = \eta(\xi), \quad u(x,t) = u(\xi), \quad \xi := x - c_s t,$$

where η and u decay to zero, along with their derivatives, as $|\xi| \to \infty$. After substituting this representation into the governing equations (2.21)-(2.22) they become:

$$\begin{aligned} -c_s\eta' + \big((d+\eta)u\big)' &= 0, \\ -c_s u' + \frac{1}{2}(u^2)' + g\eta' + c_s\frac{d^2}{3}u''' - \frac{d^2}{3}uu''' &= 0. \end{aligned}$$

An integration of the mass conservation equation and the decay at infinity lead to

$$u = \frac{c_s\eta}{d+\eta}, \qquad \eta = \frac{d\cdot u}{c_s - u}. \tag{2.23}$$

Then the momentum balance equation can be integrated once and we have

$$-c_s\Big(u-\frac{d^2}{3}u''\Big)+\frac{1}{2}u^2+\frac{gd\cdot u}{c_s-u}-\frac{d^2}{3}\Big(\frac{1}{2}(u')^2-uu''\Big)=0. \tag{2.24}$$

Similarly to the case of the (iBBM), one can see that, (2.24) written as a first order system and when $c_s^2-gd>0$, the origin is a saddle point; the phase plane sketched in Figure 2(b) also shows a solitary wave, in the form of a trajectory $O\to A\to B\to O$.

2.6. **The Serre equations.** In order to complete the presentation of our model equations, we consider the fully-nonlinear system referred to as the Serre, [68, 3, 26], or the Green–Naghdi equations, [37, 38, 42, 50, 17]:

$$h_t+[hu]_x = 0, \tag{2.25}$$

$$u_t+uu_x+gh_x = \tfrac{1}{3}\,h^{-1}\big[h^3(u_{xt}+uu_{xx}-u_x^2)\big]_x. \tag{2.26}$$

Solitary wave solutions of (2.25)-(2.26) are explicitly known. They are given by the formulas:

$$\eta(x,t)=a_0\mathrm{sech}^2\big(\tfrac{1}{2}\kappa(x-c_st-x_0)\big),\quad u=\frac{c_s\,\eta}{d+\eta},\quad c_s=\sqrt{g(d+a_0)},\quad (\kappa d)^2=\frac{3a_0}{d+a_0}. \tag{2.27}$$

As pointed out by Li, [49] and [50], the Serre equations possess a Hamiltonian structure:

$$\begin{pmatrix}h_t\\ \tilde{q}_t\end{pmatrix} = \mathbb{J}\cdot\begin{pmatrix}\delta\,\mathcal{H}\,/\,\delta h\\ \delta\,\mathcal{H}\,/\,\delta\tilde{q}\end{pmatrix},$$

where the Hamiltonian functional $\mathcal{H}$ and the operator $\mathbb{J}$ are given by

$$\mathcal{H} = \tfrac{1}{2}\int_{\mathbb{R}}\Big[\,h\,u^2+\tfrac{1}{3}\,h^3\,u_x^2+g\,\eta^2\,\Big]\,\mathrm{d}x,\qquad \mathbb{J} = -\begin{pmatrix}0 & h_x\\ h\partial_x & \tilde{q}_x+\tilde{q}\partial_x\end{pmatrix}.$$

The variable $\tilde{q}$ is sometimes referred to as the *potential vorticity flux* and is defined by

$$\tilde{q} := h\,u-\tfrac{1}{3}\,[\,h^3\,u_x\,]_x.$$

The Serre equations (2.25)-(2.26) can be shown to have the Galilean invariance property. For the mass conservation equation (2.25) we refer to Section 2.5. Thus it remains to check this property for the momentum conservation equation (2.26). If we make the change of variables $t\to t$, $x\to x-ct$, $h\to h$ and $u\to u+c$ as before, equation (2.26) becomes:

$$u_t-cu_x+(u+c)u_x+gh_x=\tfrac{1}{3}\,h^{-1}\big[h^3(u_{xt}-cu_{xx}+(u+c)u_{xx}-u_x^2)\big]_x,$$

and after two simple algebraic simplifications one can recover the original equation (2.26).

3. Numerical computation of travelling waves

In the previous section we presented several classical models arising in water wave theory. Moreover, we proposed two novel equations, the iBBM equation and the (iPer) system, with the aim of incorporating the property of invariance under the Galilean transformation, lost by the original BBM equation and the (cPer) model. The purpose of this and the next sections is to compare these models through the computation of their respective solitary

wave solutions (and whenever possible with the solitary waves of full Euler equations). Some of the models, such as the KdV, BBM and Serre equations, possess explicit formulas for these solutions, while the iBBM equation, the (iPer) system and the (cPer) system do not. Consequently, the latter have to be constructed numerically. In the next section we give the great lines of the numerical procedure to this end, as well as the method we use to construct approximate solitary waves of the Euler equations. Both techniques will be applied in the comparative study. We note that in all cases we will use the models in nondimensional but unscaled variables (taking $\varepsilon = \mu^2 = 1$).

3.1. **Computation of travelling-wave profiles. The Petviashvili method.** The investigation for travelling wave solutions in one-dimensional systems typically leads to a set of differential equations of the form

$$\mathcal{L}U = \mathcal{N}(U), \tag{3.1}$$

for some differential operators $\mathcal{L}$ (linear) and $\mathcal{N}$ (nonlinear). The numerical resolution of the preceding system can be done in many different ways (see [73] and the references therein as a modest representation of the related literature). Among all the possibilities, the so-called Petviashvili method will be used in our computations. This method stems from the pioneering work of V.I. Petviashvili (1976), [66]. It is based on a modification of the classical fixed point iteration (which in these cases is usually divergent) and it is formulated as follows. Given an initial profile U_0, the Petviashvili iteration generates approximations U_n of the original solution of (3.1) following the formulas

$$M_n = \frac{\langle \mathcal{L}U_n, U_n\rangle}{\langle \mathcal{N}(U_n), U_n\rangle}, \tag{3.2}$$

$$\mathcal{L}U_{n+1} = M_n^{\gamma} N(U_n), \tag{3.3}$$

where $\langle\cdot,\cdot\rangle$ denotes the usual L^2-norm and γ is a free parameter that controls the convergence of the method. The term (3.2) is called the stabilizing factor. See [62, 46] for details, generalizations and some local convergence results.

In this study, (3.2)-(3.3) is applied to compute solitary wave profiles in the following cases and with the corresponding operators, namely:

- (iBBM):

$$\mathcal{L}u = (\sqrt{gd} - c_s)u + c_s\frac{d^2}{6}u'', \quad \mathcal{N}(u) = \frac{d^2}{4}\left(\frac{(u')^2}{2} - uu''\right) - \frac{3}{4}u^2.$$

- (cPer):

$$\mathcal{L}u = c_s\left(u - \frac{d^2}{3}u''\right), \quad \mathcal{N}(u) = \frac{u^2}{2} + \frac{gdu}{c_s - u}.$$

- (iPer):

$$\mathcal{L}u = c_s\left(u - \frac{d^2}{3}u''\right), \quad \mathcal{N}(u) = \frac{u^2}{2} + \frac{gdu}{c_s - u} - \frac{d^2}{3}\left(\frac{(u')^2}{2} - uu''\right),$$

where c_s is the solitary wave speed.

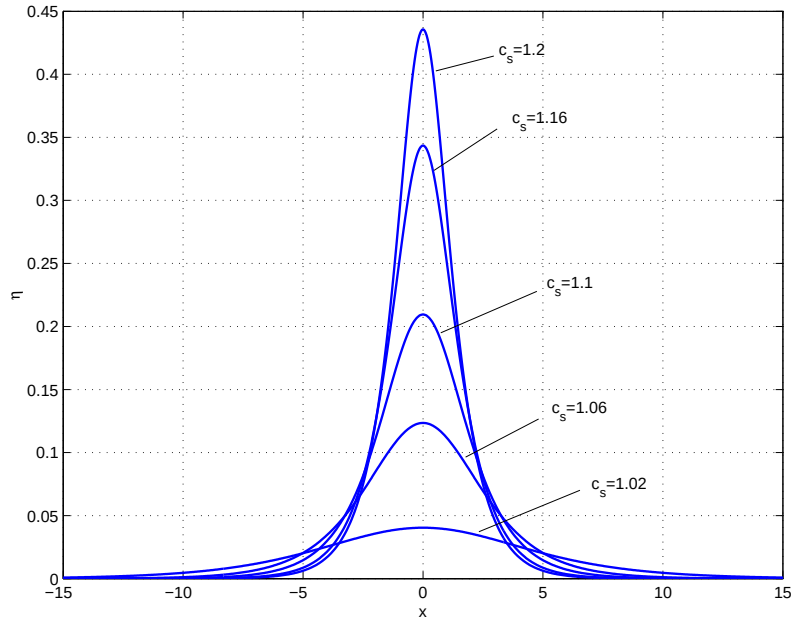

FIGURE 3. Solitary wave profiles of the invariant Benjamin–Bona–Mahony (iBBM) equation for different speeds c_s.

3.1.1. *Generation and numerical evolution of the profiles.* In many cases, the method (3.2)-(3.3) can be efficiently implemented by using Fourier techniques, [62, 46]. Specifically, our implementation for the three systems has been performed by considering the corresponding periodic problem and using a pseudospectral representation for the approximations to the profiles. As an initial iteration, a solitary wave solution (2.27) of the Serre equations or the third-order asymptotic solution of Grimshaw, [39], can be considered. The iterative procedure is continued until the difference between two consecutive iterations in the L_∞ norm, or the L_∞ norm of the residual is less than a prescribed small tolerance which, in our case, is of order $\mathcal{O}(10^{-15})$. The convergence is reached in 10–20 iterations. In order to illustrate better the transformations that solitary waves undergo while we gradually increase the propagation speed parameter c_s, we superpose several profiles on the same Figure (Figure 3 corresponds to invariant Benjamin–Bona–Mahony (iBBM) system and Figure 4 to invariant Peregrine (iPer)) system.

In order to assess the accuracy of the computations, the three models have been numerically integrated in time using the computed solitary wave profiles as the initial conditions. Some error indicators measuring the accuracy of the numerical approximation of the solitary waves have been computed. The numerical method for the corresponding initial-periodic boundary value problem consists of a pseudospectral-Galerkin method for the semi-discretization in space and the classical, explicit fourth-order Runge-Kutta scheme for the time integration, [28].

In the experiments below, we study the propagation of a solitary-wave profile, generated by (3.2)-(3.3) with speed $c_s = 1.1$ in the interval $[-128, 128]$, with $N = 2048$ points for the

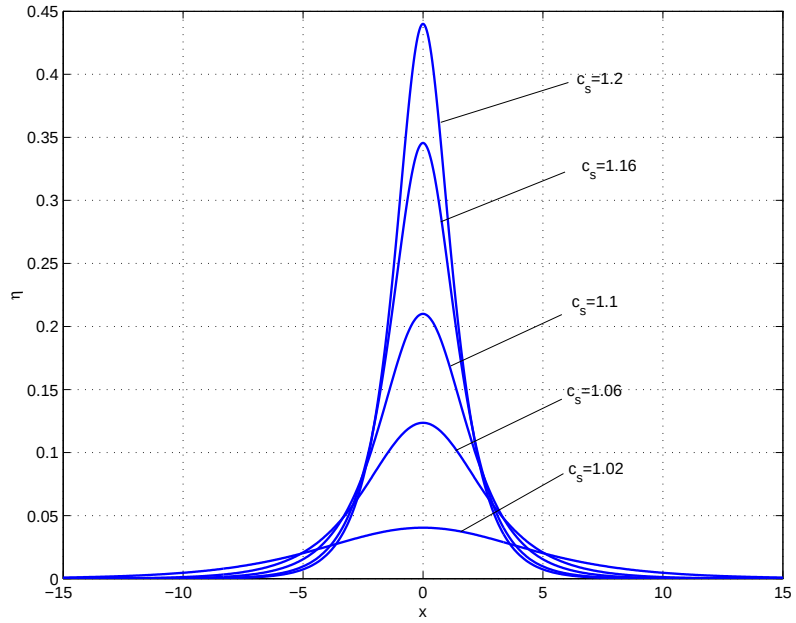

FIGURE 4. Solitary wave profiles of the invariant Peregrine (iPer) system for different speeds c_s.

pseudospectral approximation and and spatial and time step sizes $dx = 1.25 \times 10^{-2}, dt = 1.25 \times 10^{-3}$ respectively. The results correspond to (cPer) and (iPer) systems. The (iBBM) case has also implemented, with similar results.

We study the evolution of two parameters: the normalized amplitude error and the shape error. The first one is computed by comparing, at each time level, the initial amplitude of the profile (generated by the Petviashvili method) with the corresponding amplitude of the numerical solution. Their computation is implemented as in e. g. [27]. Figure 5 shows the temporal evolution of this amplitude error up to a final time $T = 100$, for both (cPer) and (iPer). We observe that for the specific values of dx and dt the amplitude is conserved up to 10 decimal digits in both cases.

On the other hand, the shape error is computed by comparing the numerical solution with time translations of the initial profile with the prescribed speed and minimizing the differences (see [9] for the details). The results displayed in Figure 6 show a virtually constant evolution of this error, which in both cases is of order $\mathcal{O}(10^{-10})$. These results confirm the accuracy of the technique used to generate the solitary wave profiles and of the numerical code for the time evolution. The latter will be used for the experiments below.

3.2. **Tanaka's solution.** The construction of approximations to travelling wave solutions for the 2D Euler equations with free surface (to be considered as reference solutions for the approximate models) will be performed with two techniques. In this Section we briefly recall some basic facts about the first one, the Tanaka's algorithm, [70]. Consider the two-dimensional water wave problem in a channel of uniform depth $d = const$. Since we look for travelling wave solutions, the flow field can be reduced to the steady state by choosing

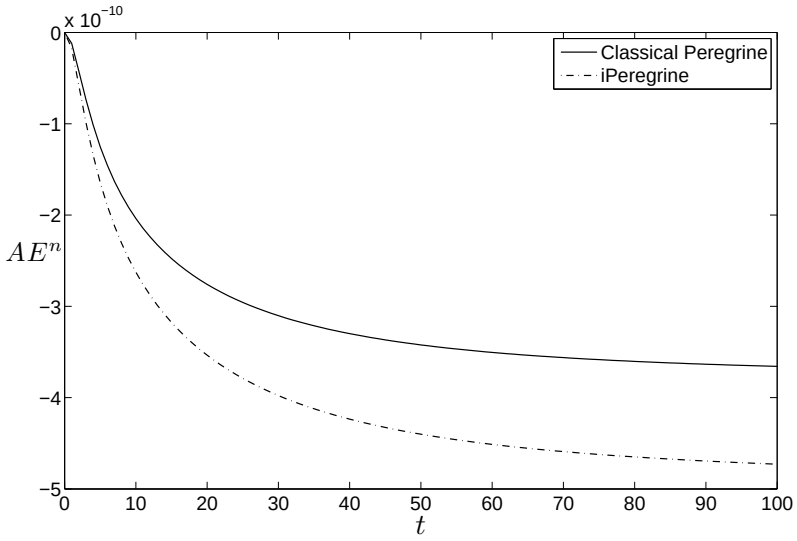

FIGURE 5. The normalized Amplitude Error as a function of time, for Peregrine and invariant Peregrine systems.

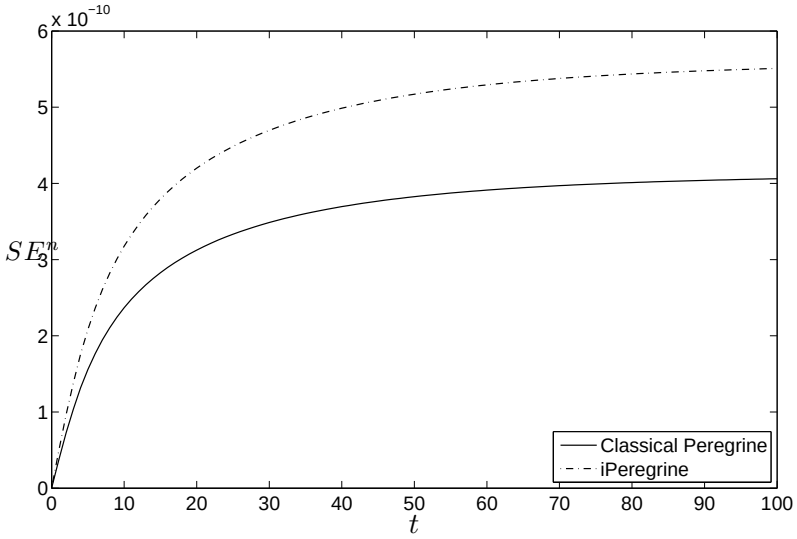

FIGURE 6. The Shape Error as a function of time, for Peregrine and invariant Peregrine systems.

a frame of reference moving with the wave speed c_s. The introduction of dimensionless variables leads to a single scaling parameter, the Froude number Fr, defined as $\mathrm{Fr} := \dfrac{c_s}{\sqrt{gd}}$. Hereafter, the governing equations are considered in dimensionless form.

The complex velocity potential is classically introduced as $w = \phi + i\psi$, where ψ is the stream function. We choose $\phi = 0$ at the crest and $\psi = 0$ at the bottom. The fluid region is then mapped onto the strip $0 < \psi < 1$, $-\infty < \phi < \infty$ on the plane w with

$\psi = 1$ corresponding to the free surface. We introduce the quantity $\Omega = \log \dfrac{dw}{dz} = \tau - i\theta$, where θ is the angle between the velocity vector and horizontal axis Ox. The real part τ is expressed in terms of the velocity magnitude q as $\tau = \log q$.

The boundary conditions to be satisfied are the dynamic condition on the free surface and the bottom impermeability; they are expressed as

$$\frac{dq^3}{d\phi} = -\frac{3}{\mathrm{Fr}^2}\sin\theta, \quad \text{on } \psi = 1 \qquad \text{and} \qquad \theta = 0, \quad \text{on } \psi = 0. \tag{3.4}$$

The problem is then transformed into the determination of the complex function Ω, analytic with respect to w within the region of the unit strip $0 < \psi < 1$, decaying at infinity and satisfying the boundary conditions (3.4). By applying Cauchy's integral theorem, one can find the following integral equation on the free surface $\psi = 1$:

$$-\theta(\phi) - \frac{2}{\pi}\int_{-\infty}^{\infty} \frac{\theta(\phi)}{(\varphi-\phi)^2+4}\,d\varphi = -\frac{1}{\pi}\int_{-\infty}^{\infty} \frac{(\varphi-\phi)\tau(\varphi)}{(\varphi-\phi)^2+4}\,d\varphi + \frac{1}{\pi}\mathrm{p.v.}\int_{-\infty}^{\infty} \frac{\tau(\varphi)}{\varphi-\phi}\,d\varphi,$$

where $\tau(\phi)$ and $\theta(\phi)$ denote the traces of the corresponding functions on the free surface $\psi = 1$. This integral equation is solved iteratively. The convergence is tested with respect to the Froude number Fr.

3.3. **Fenton's asymptotic solution.** In 1972 Fenton proposed a ninth-order asymptotic solution to the solitary wave of the full Euler equations [34]. Later, in collaboration with Longuet-Higgins, this solution was extended to the 14th order [52]. For example the 14th order approximation to the speed c_s (given the amplitude a) can be described by the following relation:

$$\left(\frac{c_s}{\sqrt{gd}}\right)^2 = \sum_{n=0}^{N} f_n \varepsilon^n + \mathcal{O}(\varepsilon^{N+1}), \qquad \varepsilon := \frac{a}{d}. \tag{3.5}$$

The coefficients f_n up to the 14th order are given in Table 1. This and the ninth-order asymptotic solutions will be also considered as reference solutions.

3.4. **Numerical results.** In this section we compare the solitary waves of the following models:

- the Korteweg–de Vries (KdV) equation (2.5)
- the Benjamin–Bona–Mahony (BBM) equation (2.9)
- the invariant Benjamin–Bona–Mahony (iBBM) equation (2.11)
- the Peregrine classical Peregrine (cPer) system (2.18), (2.19)
- the invariant Peregrine invariant Peregrine (iPer) system (2.21), (2.22)
- the Serre equations (2.25), (2.26)

from either the analytical formula (when possible) or the computations with the Petviashvili method. The comparison is established between them and with those of the full Euler equations with free surface. The latter are computed by two ways: from the Fenton

Order, n	Coefficient value, f_n
0	1.000000
1	1.000000
2	-0.050000
3	-0.0428571
4	-0.0342857
5	-0.0315195
6	-0.0292784
7	-0.0268451
8	-0.0302634
9	-0.0219347
10	-0.048229
11	0.051809
12	-0.506790
13	3.4666
14	-31.64

TABLE 1. Coefficients of the Fenton's asymptotic expansion of the solitary wave speed, cf. [34, 52].

asymptotic ninth order solution and the Tanaka's solution of the two-dimensional incompressible Euler equations with free surface. The study is focused on the amplitudes and shapes of the computed free surface elevation $\eta(\xi)$, provided by the models for the same prescribed value of the propagation speed parameter c_s.

3.4.1. *Solitary wave speed–amplitude relation.* Figure 7 shows an amplitude-wave speed diagram for the models considered. First, an approximate relation between the amplitude and speed for the solitary waves of the full Euler system is computed, by using the Tanaka's algorithm and (3.5). They virtually give the same results and these are compared with the relation obtained by each of the models. We observe that the Serre equations (and, consequently, the other systems, that have weaker nonlinearities) are known to provide a relatively good approximation to solitary wave solutions of full Euler equations in a range of amplitudes not greater than 0.5, cf. e.g. [51, 16]. Therefore, our attention is focused on solitary waves with these amplitudes, as it is observed in Figure 7. Figure 8 shows a magnification for the largest amplitudes.

Corresponding to the comparison between the solitary waves of the models at hand, we note that the non Galilean invariant models, the Benjamin–Bona–Mahony (BBM) equation and the classical Peregrine (cPer) system, tend to underestimate the solution speed for a given amplitude. On the other hand, the curves corresponding to their invariant counterparts along with the fully nonlinear Serre equations lie above the reference solution. In particular, the results for the invariant Benjamin–Bona–Mahony (iBBM) equation are very close to those of Serre equations. A surprising fact is that the amplitude-speed

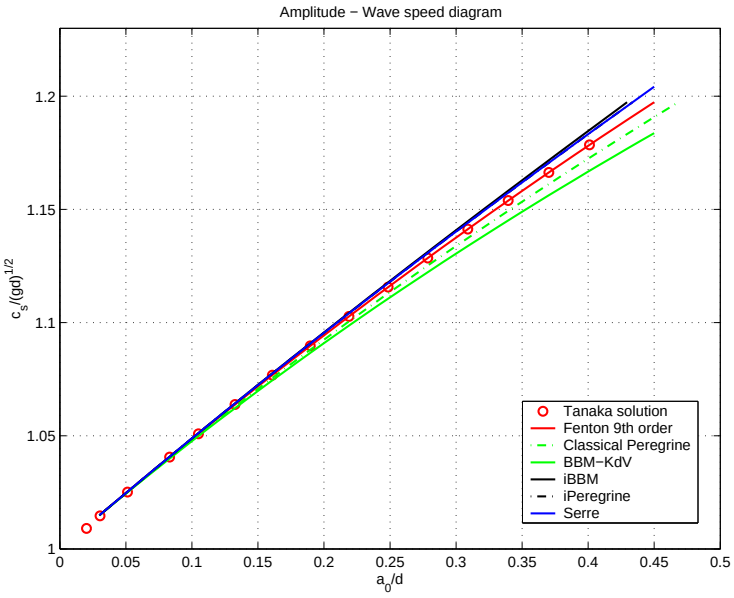

FIGURE 7. Solitary wave amplitude–speed diagram. (The curves corresponding to the iPeregrine system and the Serre system are superposed up to the graphical resolution.)

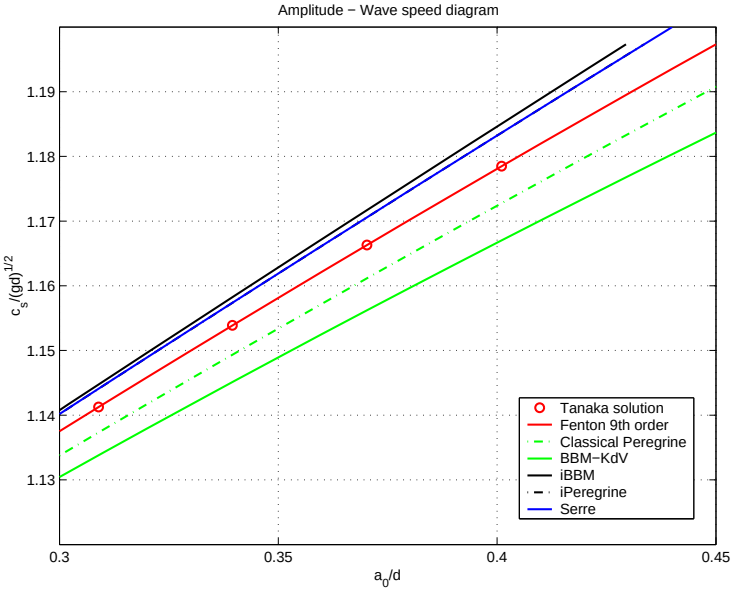

FIGURE 8. Magnification of Figure 7. (The curves corresponding to the iPeregrine system and the Serre system are superposed up to the graphical resolution.)

relation given by the invariant Peregrine (iPer) system is superposed with that of the Serre equations up to the graphical resolution.

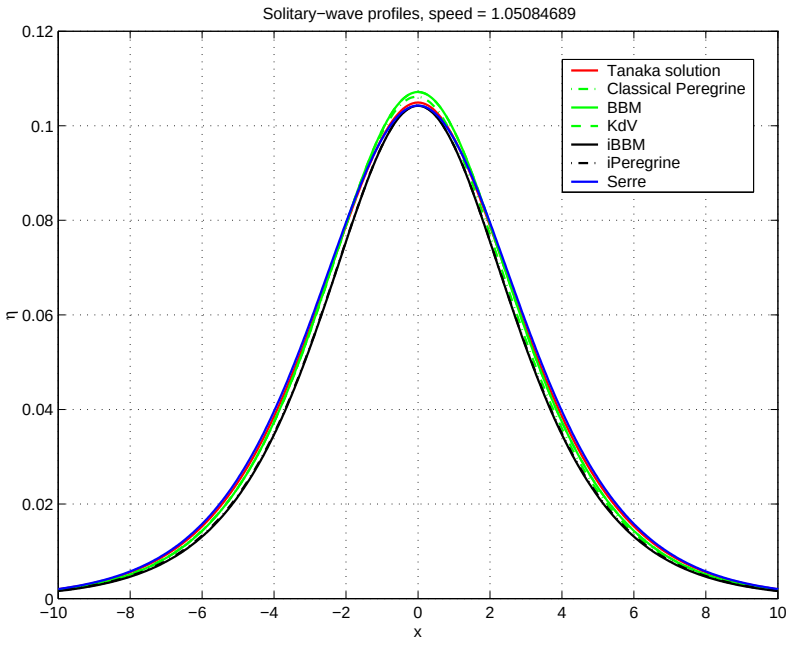

FIGURE 9. Small amplitude solitary waves computed for the propagation speed $\frac{c_s}{\sqrt{gd}} = 1.05084689$ $(a/d \approx 0.1)$.

3.4.2. *Solitary wave shapes.* A second comparison between the shape of the computed solitary waves, is presented in Figures 9-14. They illustrate the cases of small $(a/d \approx 0.1$, see Figure 9 and a magnification on the wave crest in Figure 10), moderate $(a/d \approx 0.22$, see Figures 11 and a magnification in Figure 12) and large $(a/d \approx 0.4$, see Figures 13 and 14) solitary wave amplitudes of the models (within the range mentioned above). According to these results, it is observed that the invariant Benjamin–Bona–Mahony (iBBM) equation and the invariant Peregrine (iPer) system approximate much better the amplitude of the reference solution (represented, in this case, by the Tanaka's solution) than the non-Galilean invariant counterparts, and they stay very close to the results of the Serre system near the crest. As a measure of the level of approximation to solitary wave solutions of the Euler system, these and the previous results show the benefits of taking into account the invariantization process in the approximate models.

4. Solitary waves interactions

We complete the numerical experiments by studying the effects of the Galilean invariance property in solitary wave interactions. Specifically, we compare, by numerical means, head-on and overtaking collisions of two solitary waves of the invariant BBM and Peregrine equations with those of their corresponding not invariant models.

It is known that the tails produced by the interaction of two solitary waves are sensitive to both the linear terms (characterizing the linear dispersion relation) and the nonlinearities. For example, two solitary waves of the KdV equation interact in an elastic way without

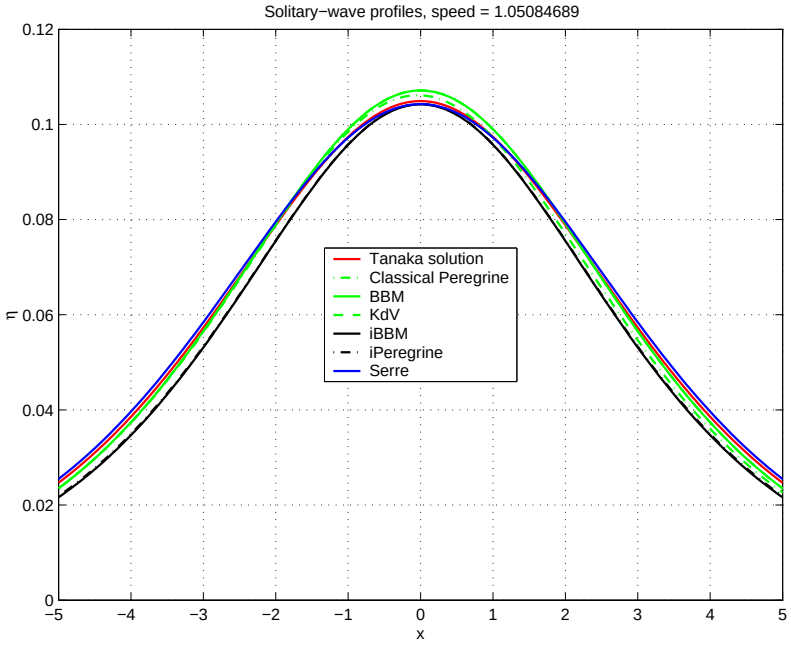

FIGURE 10. Magnification of Figure 9.

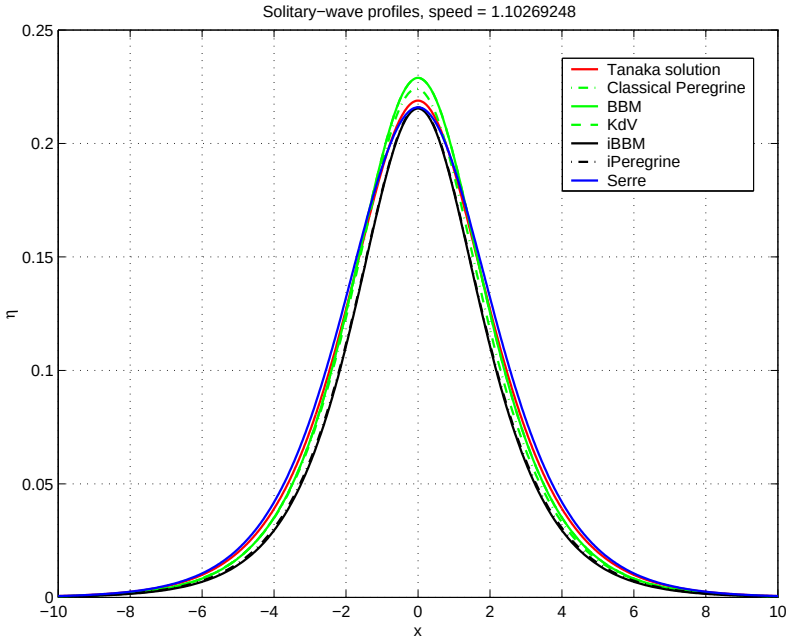

FIGURE 11. Moderate amplitude solitary waves computed for the propagation speed $\frac{c_s}{\sqrt{gd}} = 1.10269248$ $(a/d \approx 0.22)$.

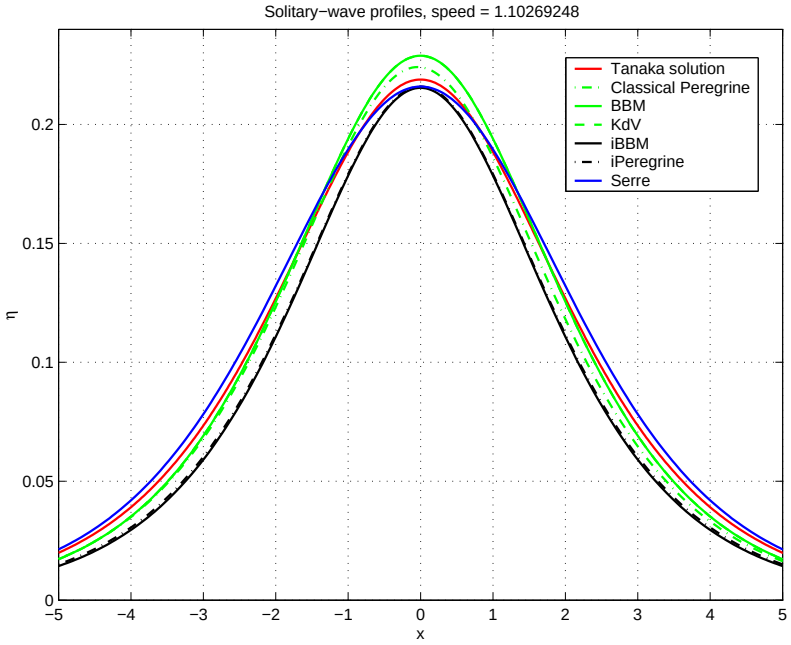

FIGURE 12. Magnification of Figure 11.

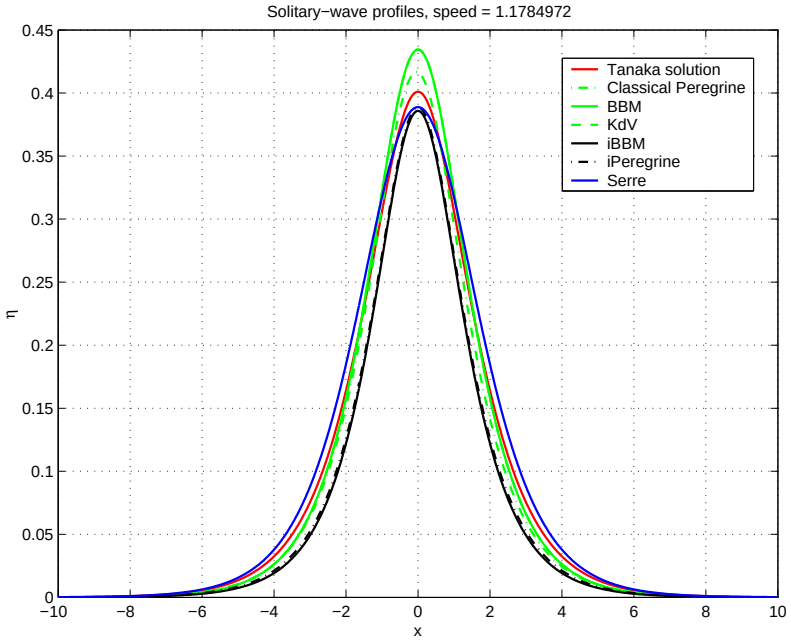

FIGURE 13. Large amplitude solitary waves computed for the propagation speed $\frac{c_s}{\sqrt{gd}} = 1.1784972$ $(a/d \approx 0.4)$.

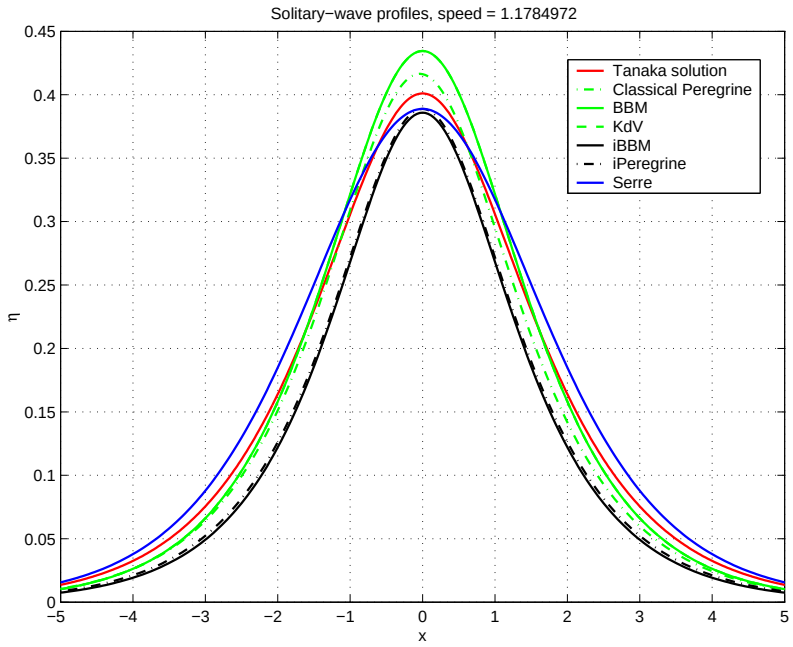

FIGURE 14. Magnification of Figure 13.

producing dispersive tails at all, [74], while the collision of solitary waves of the BBM equation will produce dispersive tails and probably small-amplitude nonlinear pulses as the main indication of an inelastic interaction, [10, 11]. In the new Galilean invariant models, the new nonlinear terms are of order $\varepsilon\mu^2$ and their effects on the interaction will be studied here. The same code introduced in Section 3 is used for the numerical computations, as well as the Petviashvili method (3.2)-(3.3) to generate solitary wave profiles when necessary.

4.1. **Head-on collisions of solitary waves.** A first group of experiments concerns head-on collisions. The classical Peregrine (cPer) and the invariant Peregrine (iPer) systems have been considered, by constructing, in both cases, two solitary waves on the interval $[-256, 256]$ with speeds $c_{s,1} = 1.15$ and $c_{s,2} = 1.05$ (translated appropriately such as their amplitudes achieved on -50 and 50 respectively) and travelling in opposite directions. These solitary waves are of small amplitude and their shapes are almost the same for both models. The code uses $N = 4096$ nodes, a spatial step size of 1.25×10^{-1} and 5×10^{-3} as the time step.

Figure 16 shows the $\eta-$ evolution of the head-on collision for both models and at several times. A tail behind each tallest wave after the collision is observed. This is larger in the case of the invariant Peregrine system (of the order of 10^{-4}) than in the case of the classical Peregrine system (approx. 10^{-4}), see Figure 16 (d) and (f). During the collisions, a similar phase shift also takes place, see Figure 17.

A final comparison is established in terms of the degree of inelasticity of the interaction. This can be measured by using several parameters, [1, 21]. In each case, a symmetric head-on collision has been implemented; that is, two solitary waves with the same spped

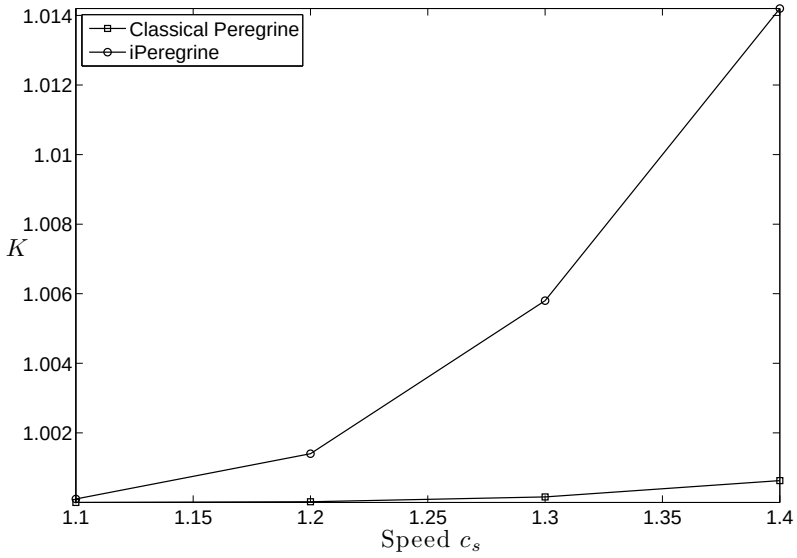

FIGURE 15. Symmetric head-on collision. Ratio K of amplitudes before and after the collision, for Peregrine and invariant Peregrine systems.

(a) Peregrine system

c_s	A_{init}	A_{after}
1.1	0.2177418	0.2177417
1.2	0.4757297	0.4757202
1.3	0.7822906	0.7821674
1.4	1.1476304	1.1469096

(b) iPeregrine system

c_s	A_{init}	A_{after}
1.1	0.21	0.209978
1.2	0.44	0.439365
1.3	0.69	0.686027
1.4	0.95	0.946593

TABLE 2. Symmetric head-on collision.

c_s travelling in opposite directions. After the interaction, both solitary waves emerge with similar amplitudes A_{after}, but below the initial one A_{init}, as is observed in Table 2. Then a ratio K of the amplitude of the waves after the collision to their amplitude before the collision has been computed. Figure 15 shows the behavior of this value, as a function of the speed parameter c_s and for both systems. The results reveal a higher inelastic collision in the case of the invariant system, in accordance to what is observed in the full water wave model [22].

4.2. **Overtaking interactions of solitary waves.** In order to study the overtaking collision of solitary waves, we first consider the classical and the invariant Peregrine systems and construct, for both, two solitary waves on the interval $[-1024, 1024]$ with speeds $c_{s,1} = 1.15$ and $c_{s,2} = 1.05$ (translated appropriately such as their amplitude achieved on -50 and 50 respectively) travelling in the same direction, with $N = 16384$ and time step of 5×10^{-3}. In Figure 18 we observe that the basic characteristics of the interaction are similar for both systems, (cf. also [2]). Specifically, the interaction is again inelastic; after the collision a

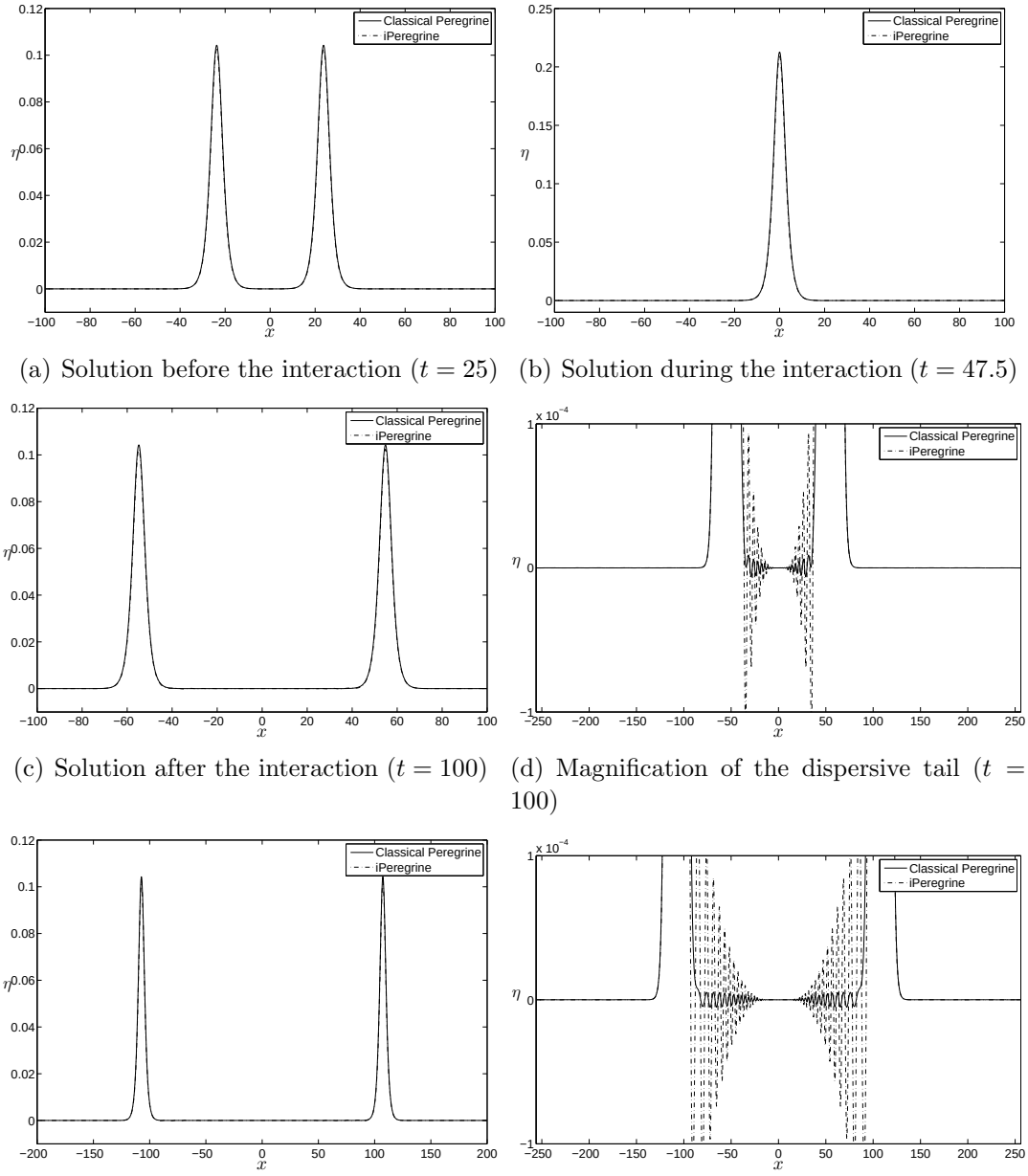

(a) Solution before the interaction ($t = 25$)

(b) Solution during the interaction ($t = 47.5$)

(c) Solution after the interaction ($t = 100$)

(d) Magnification of the dispersive tail ($t = 100$)

(e) Solution after the interaction ($t = 150$)

(f) Magnification of the dispersive tail ($t = 150$)

FIGURE 16. Head on collision of two solitary waves for the Peregrine and invariant Peregrine systems.

tail, of apparent dispersive nature, behind the smallest wave (moving to the right) and a small N-shape wavelet (moving to the left) are generated. Moreover, a small phase shift and a change in shape can be observed in the solitary pulses (Figure 17). The wavelet

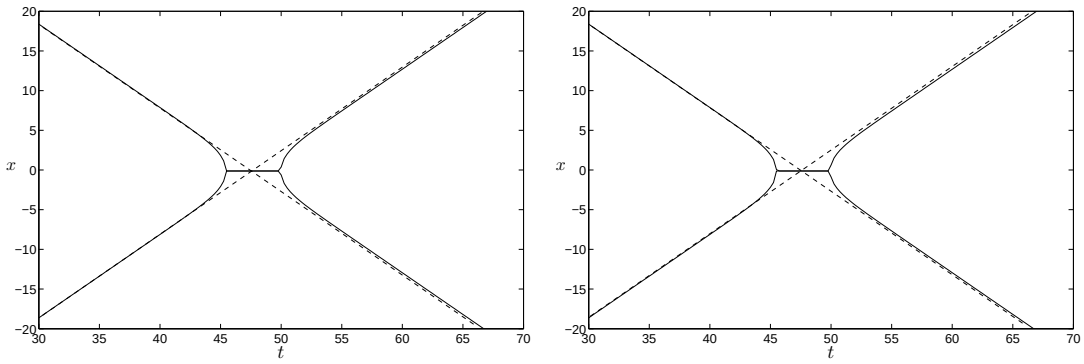

(a) (b)

FIGURE 17. Phase diagram of the overtaking collision: (a) Peregrine system. (b) Invariant Peregrine system.

generated in the case of the classical Peregrine system has an inverse N-shape while the invariant version has an N-shape.

On the contrary, with the same input data, an overtaking collision for the case of the BBM and iBBM equations is shown in Figure 19 at several times. In this case, no N-shape wavelet is observed and only a tail behind the waves appears.

We can conclude that these two groups of results show that, as expected, the $\mathcal{O}(\epsilon\mu^2)$ nonlinear terms of the invariant models do not change significantly, in a qualitative sense, the behaviour of the interactions of solitary waves provided by the corresponding not Galilean invariant system.

4.3. **Comparison with Euler equations.** Finally, we study the evolution of a solitary wave of the Euler equations when we use it as initial condition to the approximate models. Specifically, we consider an approximate solitary wave $\Phi_h(x)$ of amplitude $A = 0.2$ (and speed $c_s \approx 1.095490471188718$) obtained by using Fenton's ninth order asymptotic solution. In the case of the Peregrine and the iPeregrine systems we use for initial velocity $u_0(x) = c_s\eta_0(x)/(d+\eta_0(x))$. We remind that due to the mass conservation property this formula is exact (see equation (2.23) for the velocity given the surface elevation η for both Peregrine and iPeregrine systems). In Figure 20 we present the solution at $T = 100$. We observe that the initial condition is resolved into a new solitary wave followed by a dispersive tail. In the case of the classical models, the dispersive tails appear to be smaller. Figure 21 (a) shows the shaper error of the solution (i.e. how much different is the solution for being the exact solitary wave of the Euler equations) while Figure 21 (b) presents the amplitude of the solution as a function of time t. From these two figures we observe that in the case of classical models the emerging solitary waves are closer in shape and amplitude to the original solitary wave solution of the Euler equations than the respective solitary waves of the invariant models.

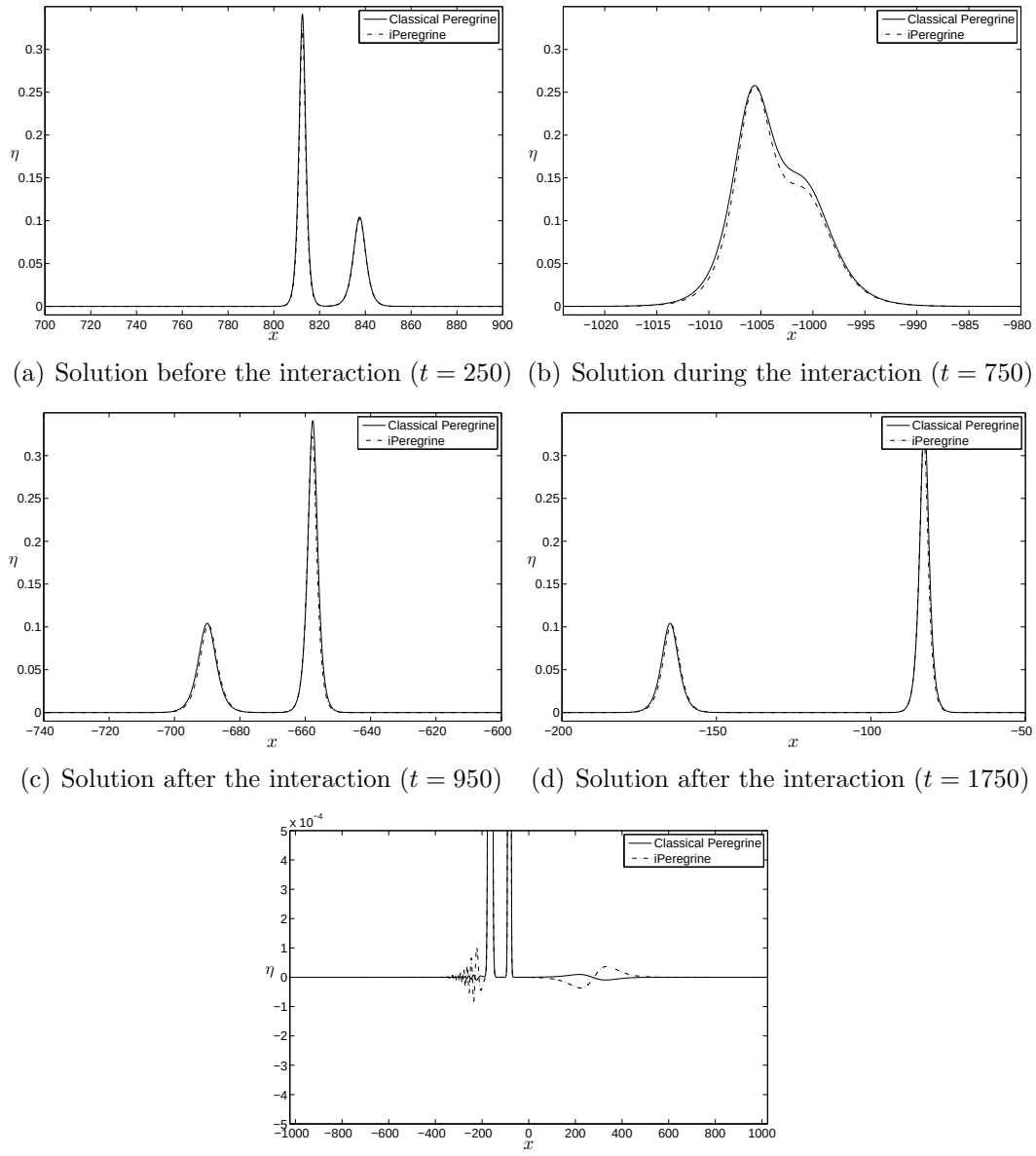

(a) Solution before the interaction ($t = 250$)

(b) Solution during the interaction ($t = 750$)

(c) Solution after the interaction ($t = 950$)

(d) Solution after the interaction ($t = 1750$)

(e) Magnification of the dispersive tail ($t = 1750$)

FIGURE 18. Overtaking collision of two solitary waves for classical Peregrine (cPer) and invariant Peregrine (iPer) systems.

5. Conclusions

In the present work the influence of Galilean invariance in several equations arising in water wave modelling is studied. We propose the modification of existing not invariant models in order to include this fundamental property. The technique introduced here consists of adding higher-order terms from the approximation of the governing equations.

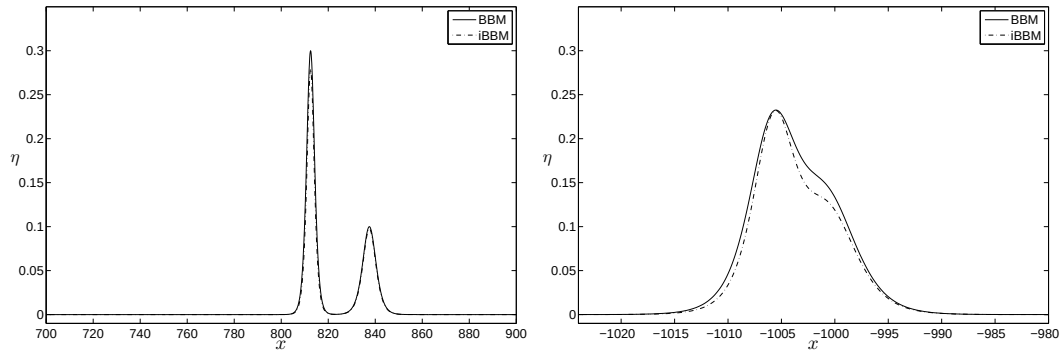

(a) Solution before the interaction ($t = 250$) (b) Solution during the interaction ($t = 750$)

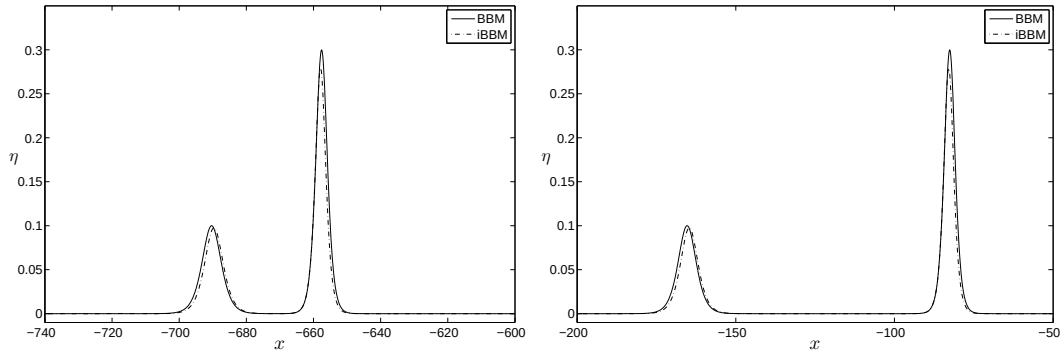

(c) Solution after the interaction ($t = 950$) (d) Solution after the interaction ($t = 1750$)

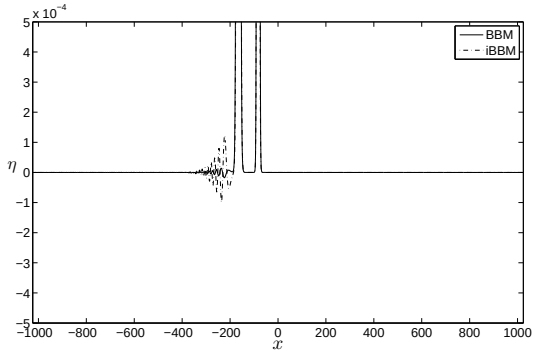

(e) Magnification of the dispersive tail ($t = 1750$)

FIGURE 19. Overtaking collision of two solitary waves for Benjamin–Bona–Mahony (BBM) and invariant Benjamin–Bona–Mahony (iBBM) models.

These terms are asymptotically negligible and consequently, the modified models are still valid in the appropriate regime. As a case study, corresponding modifications of two not invariant models, the Benjamin–Bona–Mahony (BBM) equation and the classical Peregrine system, are presented. The comparison with reference solutions to the full Euler equations shows that this extra-term is beneficial for the description of the travelling wave solutions

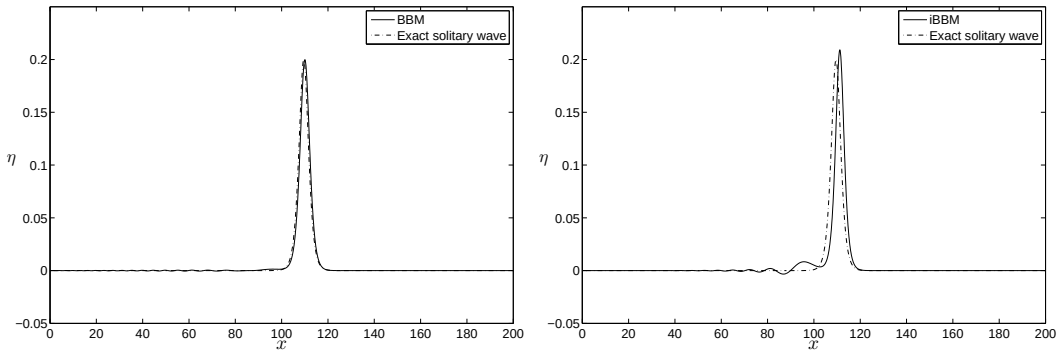

(a) Solution of the BBM equation at $T = 100$ (b) Solution of the iBBM equation at $T = 100$

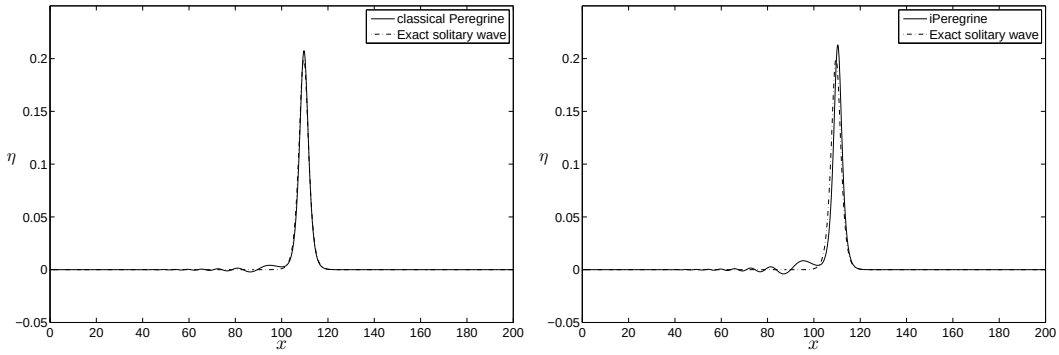

(c) Solution of the Peregrine system at $T = 100$ (d) Solution of the iPeregrine system at $T = 100$

FIGURE 20. Evolution of a solitary wave of the Euler equations. ($A = 0.2$)

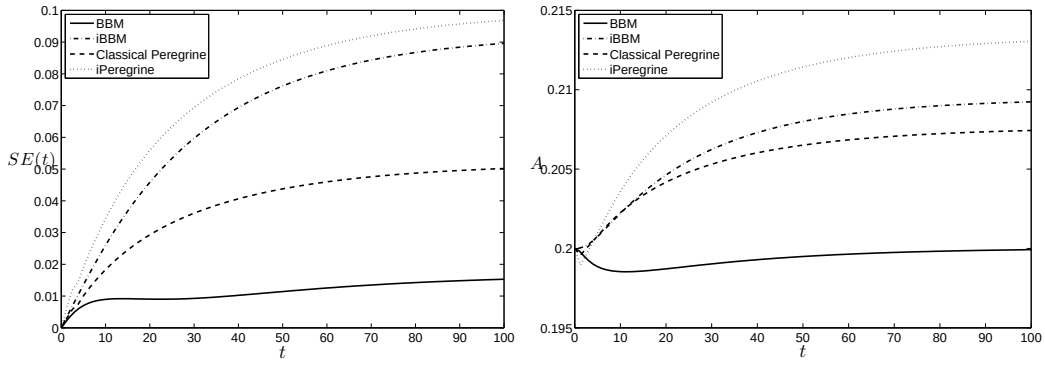

(a) Shape error (b) Amplitude

FIGURE 21. Shape error and amplitude of the solution as a function of time

in several ways. First, this modification improves the SW amplitude-speed relation which lies closer to the Tanaka's and Fenton's solutions. In this regard, we obtain a surprising performance of the iPeregrine system (2.21), (2.22) with the amplitude-speed relation

undistinguishable from the fully-nonlinear Serre equations (2.25), (2.26). Moreover, the amplitudes of solitary wave solutions to the invariant models are closer to the corresponding full Euler solutions than classical counterparts. The comparison is finished off with a numerical study of head-on and overtaking collisions. Compared to the behaviour observed in the not invariant equations, the higher order nonlinear terms incorporated in the new models do not affect qualitatively the inelastic character of the interactions. However, a relevant difference in the degree of inelasticity is observed, being higher in the case of the invariant versions. This behaviour is closer to what has been observed in the case of the full Euler equations.

Acknowledgements

D. Dutykh acknowledges the support from French Agence Nationale de la Recherche, project MathOcéan (Grant ANR-08-BLAN-0301-01) and the support from the University of Valladolid during his stay in July, 2011. A. Duran has been supported by MICINN project MTM2010-19510/MTM.

The authors would like to thank Professors Didier Clamond, Vassilios Dougalis and Cesar Palencia for very helpful discussions.

References

[1] K. O. Abdulloev, I. L. Bogolubsky, and V. G. Makhankov. One more example of inelastic soliton interaction. *Phys. Lett.*, 56A:1976, 1976. 21

[2] D. C. Antonopoulos, V. A. Dougalis, and D. E. Mitsotakis. Numerical solution of Boussinesq systems of the Bona-Smith family. *Appl. Numer. Math.*, 30:314–336, 2010. 22

[3] E. Barthélémy. Nonlinear shallow water theories for coastal waves. *Surveys in Geophysics*, 25:315–337, 2004. 10

[4] T. B. Benjamin, J. L. Bona, and J. J. Mahony. Model equations for long waves in nonlinear dispersive systems. *Philos. Trans. Royal Soc. London Ser. A*, 272:47–78, 1972. 5

[5] T. B. Benjamin and P. Olver. Hamiltonian structure, symmetries and conservation laws for water waves. *J. Fluid Mech*, 125:137–185, 1982. 2, 3

[6] O. Bokhove. Flooding and Drying in Discontinuous Galerkin Finite-Element Discretizations of Shallow-Water Equations. Part 1: One Dimension. *Journal of Scientific Computing*, 22-23:47–82, 2005. 2

[7] J. L. Bona and M. Chen. A Boussinesq system for two-way propagation of nonlinear dispersive waves. *Physica D*, 116:191–224, 1998. 2

[8] J. L. Bona, M. Chen, and J.-C. Saut. Boussinesq equations and other systems for small-amplitude long waves in nonlinear dispersive media. I: Derivation and linear theory. *Journal of Nonlinear Science*, 12:283–318, 2002. 2, 4, 8

[9] J. L. Bona, V. A. Dougalis, and D. E. Mitsotakis. Numerical solution of KdV-KdV systems of Boussinesq equations: I. The numerical scheme and generalized solitary waves. *Mat. Comp. Simul.*, 74:214–228, 2007. 13

[10] J. L. Bona, W. G. Pritchard, and L. R. Scott. Solitary-wave interaction. *Phys. Fluids*, 23:438–441, 1980. 21

[11] J. L. Bona, W. G. Pritchard, and L. R. Scott. An Evaluation of a Model Equation for Water Waves. *Phil. Trans. R. Soc. Lond. A*, 302:457–510, 1981. 21

[12] J. L. Bona and R. Smith. A model for the two-way propagation of water waves in a channel. *Math. Proc. Camb. Phil. Soc.*, 79:167–182, 1976. 2, 4

[13] J. Boussinesq. Théorie des ondes et des remous qui se propagent le long d'un canal rectangulaire horizontal, en communiquant au liquide contenu dans ce canal des vitesses sensiblement pareilles de la surface au fond. *J. Math. Pures Appl.*, 17:55–108, 1872. 4

[14] L. J. F. Broer. On the Hamiltonian theory of surface waves. *Applied Sci. Res.*, 29(6):430–446, 1974. 3

[15] R. Camassa and D. Holm. An integrable shallow water equation with peaked solitons. *Phys. Rev. Lett.*, 71(11):1661–1664, 1993. 7

[16] J. D. Carter and R. Cienfuegos. The kinematics and stability of solitary and cnoidal wave solutions of the Serre equations. *Eur. J. Mech. B/Fluids*, 30:259–268, 2011. 16

[17] F. Chazel, D. Lannes, and F. Marche. Numerical simulation of strongly nonlinear and dispersive waves using a Green-Naghdi model. *J. Sci. Comput.*, 48:105–116, 2011. 2, 10

[18] M. Chhay, E. Hoarau, A. Hamdouni, and P. Sagaut. Comparison of some Lie-symmetry-based integrators. *J. Comp. Phys.*, 230(5):2174–2188, 2011. 2

[19] C. I. Christov. An energy-consistent dispersive shallow-water model. *Wave Motion*, 34:161–174, 2001. 2, 6

[20] D. Clamond and D. Dutykh. Practical use of variational principles for modeling water waves. *Physica D: Nonlinear Phenomena*, 241(1):25–36, 2012. 2, 3

[21] J. Courtenay Lewis and J. A. Tjon. Resonant production of solitons in the RLW equation. *Phys. Lett.*, 73A:275–279, 1979. 21

[22] W. Craig, P. Guyenne, J. Hammack, D. Henderson, and C. Sulem. Solitary water wave interactions. *Phys. Fluids*, 18(5):57106, 2006. 22

[23] A. D. D. Craik. The origins of water wave theory. *Ann. Rev. Fluid Mech.*, 36:1–28, 2004. 3

[24] A. J. C. de Saint-Venant. Théorie du mouvement non-permanent des eaux, avec application aux crues des rivières et à l'introduction des marées dans leur lit. *C. R. Acad. Sc. Paris*, 73:147–154, 1871. 2

[25] A. Degasperis and M. Procesi. *Symmetry and Perturbation Theory*, chapter Asymptotic, pages 23–37. World Scientific, 1999. 7

[26] F. Dias and P. Milewski. On the fully-nonlinear shallow-water generalized Serre equations. *Physics Letters A*, 374(8):1049–1053, 2010. 2, 10

[27] V. Dougalis, A. Duran, M. A. Lopez-Marcos, and D. E. Mitsotakis. A numerical study of the stability of solitary waves of Bona-Smith family of Boussinesq systems. *J. Nonlinear Sci.*, 17:595–607, 2007. 13

[28] V. A. Dougalis and D. E. Mitsotakis. Theory and numerical analysis of Boussinesq systems: A review. In N A Kampanis, V A Dougalis, and J A Ekaterinaris, editors, *Effective Computational Methods in Wave Propagation*, pages 63–110. CRC Press, 2008. 12

[29] D. Dutykh and D. Clamond. Shallow water equations for large bathymetry variations. *J. Phys. A: Math. Theor.*, 44(33):332001, 2011. 2

[30] D. Dutykh and F. Dias. Dissipative Boussinesq equations. *C. R. Mecanique*, 335:559–583, 2007. 4

[31] D. Dutykh, Th. Katsaounis, and D. Mitsotakis. Finite volume schemes for dispersive wave propagation and runup. *J. Comput. Phys*, 230:3035–3061, 2011. 2

[32] D. Dutykh and D. Mitsotakis. On the relevance of the dam break problem in the context of nonlinear shallow water equations. *Discrete and Continuous Dynamical Systems - Series B*, 13(4):799–818, 2010. 2

[33] D. Dutykh, R. Poncet, and F. Dias. The VOLNA code for the numerical modeling of tsunami waves: Generation, propagation and inundation. *Eur. J. Mech. B/Fluids*, 30(6):598–615, 2011. 2

[34] J. Fenton. A ninth-order solution for the solitary wave. *J. Fluid Mech*, 53(2):257–271, 1972. 15, 16

[35] R. Fetecau and D. Levy. Aproximate model equations for water waves. *Comm. Math. Sci.*, 3:159–170, 2005. 7

[36] C. S. Gardner, J. M. Greene, M. D. Kruskal, and R. M. Miura. Korteweg-de Vries equation and Generalizations. VI. Methods for Exact Solution. *Comm. Pure Appl. Math.*, 27:97–133, 1974. 4

[37] A. E. Green, N. Laws, and P. M. Naghdi. On the theory of water waves. *Proc. R. Soc. Lond. A*, 338:43–55, 1974. 2, 10

[38] A. E. Green and P. M. Naghdi. A derivation of equations for wave propagation in water of variable depth. *J. Fluid Mech.*, 78:237–246, 1976. 2, 10

[39] R. Grimshaw. The solitary wave in water of variable depth. Part 2. *J. Fluid Mech*, 46:611–622, 1971. 12

[40] R. S. Johnson. *A Modern Introduction to the Mathematical Theory of Water Waves*. Cambridge University Press, 2004. 4

[41] U. Kanoglu and C. Synolakis. Initial Value Problem Solution of Nonlinear Shallow Water-Wave Equations. *Phys. Rev. Lett.*, 97:148501, 2006. 2

[42] J. W. Kim, K. J. Bai, R. C. Ertekin, and W. C. Webster. A derivation of the Green-Naghdi equations for irrotational flows. *Journal of Engineering Mathematics*, 40(1):17–42, 2001. 2, 10

[43] P. Kim. Invariantization of numerical schemes using moving frames. *BIT Numerical Mathematics*, 47:525–546, 2007. 2

[44] P. Kim. Invariantization of the Crank-Nicolson method for Burgers' equation. *Physica D*, 237:243–254, 2008. 2

[45] D. J. Korteweg and G. de Vries. On the change of form of long waves advancing in a rectangular canal, and on a new type of long stationary waves. *Phil. Mag.*, 39(5):422–443, 1895. 4

[46] T. I. Lakoba and J. Yang. A generalized Petviashvili iteration method for scalar and vector Hamiltonian equations with arbitrary form of nonlinearity. *J. Comp. Phys.*, 226:1668–1692, 2007. 11, 12

[47] H. Lamb. *Hydrodynamics*. Cambridge University Press, 1932. 3

[48] P. D. Lax. Integrals of nonlinear equations of evolution and solitary waves. *Commun. Pure Appl. Math.*, 21:467–490, 1968. 4

[49] Y. A. Li. Linear stability of solitary waves of the Green-Naghdi equations. *Commun. Pure Appl. Math.*, 54(5):501–536, 2001. 10

[50] Y. A. Li. Hamiltonian structure and linear stability of solitary waves of the Green-Naghdi equations. *J. Nonlin. Math. Phys.*, 9(1):99–105, 2002. 10

[51] Y. A. Li, J. M. Hyman, and W. Choi. A Numerical Study of the Exact Evolution Equations for Surface Waves in Water of Finite Depth. *Stud. Appl. Maths.*, 113:303–324, 2004. 16

[52] M. Longuet-Higgins and J. Fenton. On the Mass, Momentum, Energy and Circulation of a Solitary Wave. II. *Proc. R. Soc. A*, 340(1623):471–493, 1974. 15, 16

[53] J. C. Luke. A variational principle for a fluid with a free surface. *J. Fluid Mech.*, 27:375–397, 1967. 3

[54] F. Marche. Derivation of a new two-dimensional viscous shallow water model with varying topography, bottom friction and capillary effects. *European Journal of Mechanics - B/Fluids*, 26(1):49–63, 2007. 2

[55] C. C. Mei. *The applied dynamics of ocean surface waves*. World Scientific, 1994. 3

[56] R. M. Miura. The Korteweg-de Vries equation: a survey of results. *SIAM Rev*, 18:412–459, 1976. 4

[57] I. Newton. *Philosophiae Naturalis Principia Mathematica*. 1687. 2

[58] O. Nwogu. Alternative form of Boussinesq equations for nearshore wave propagation. *J. Waterway, Port, Coastal and Ocean Engineering*, 119:618–638, 1993. 2, 4

[59] P. J. Olver. *Applications of Lie groups to differential equations*, volume 107 (2nd e of *Graduate Texts in Mathematics*. Springer-Verlag, 1993. 2

[60] P. J. Olver. Personal web page, 2012. 7

[61] R. L. Pego and M. I. Weinstein. Convective linear stability of solitary waves for Boussinesq equations. *Stud. Appl. Maths.*, 99:311–375, 1997. 8

[62] D. Pelinovsky and Y. A. Stepanyants. Convergence of Petviashvili's iteration method for numerical approximation of stationary solutions of nonlinear wave equations. *SIAM J. Num. Anal.*, 42:1110–1127, 2004. 11, 12

[63] D. H. Peregrine. Calculations of the development of an undual bore. *J. Fluid Mech.*, 25:321–330, 1966. 5

[64] D. H. Peregrine. Long waves on a beach. *J. Fluid Mech.*, 27:815–827, 1967. 4, 8
[65] A. A. Petrov. Variational statement of the problem of liquid motion in a container of finite dimensions. *Prikl. Math. Mekh.*, 28(4):917–922, 1964. 3
[66] V. I. Petviashvili. Equation of an extraordinary soliton. *Sov. J. Plasma Phys.*, 2(3):469–472, 1976. 11
[67] R. Salmon. Hamiltonian fluid mechanics. *Ann. Rev. Fluid Mech.*, 20:225–256, 1988. 3
[68] F. Serre. Contribution à l'étude des écoulements permanents et variables dans les canaux. *La Houille blanche*, 8:374–872, 1953. 2, 10
[69] J. J. Stoker. *Water waves, the mathematical theory with applications*. Wiley, 1958. 3
[70] M. Tanaka. The stability of solitary waves. *Phys. Fluids*, 29(3):650–655, 1986. 13
[71] F. Ursell. The long-wave paradox in the theory of gravity waves. *Proc. Camb. Phil. Soc.*, 49:685–694, 1953. 5
[72] G. B. Whitham. *Linear and nonlinear waves*. John Wiley & Sons Inc., New York, 1999. 3
[73] J. Yang. *Nonlinear Waves in Integrable and Nonintegrable Systems*. SIAM, 2010. 11
[74] N. J. Zabusky and M. D. Kruskal. Interaction of solitons in a collisionless plasma and the recurrence of initial states. *Phys. Rev. Lett*, 15:240–243, 1965. 21
[75] V. E. Zakharov. Stability of periodic waves of finite amplitude on the surface of a deep fluid. *J. Appl. Mech. Tech. Phys.*, 9:1990–1994, 1968. 3

Departamento de Matemática Aplicada, E.T.S.I. Telecomunicación, Campus Miguel Delibes, Universidad de Valladolid, Paseo de Belen 15, 47011 Valladolid, Spain
E-mail address: angel@mac.uva.es

LAMA, UMR 5127 CNRS, Université de Savoie, Campus Scientifique, 73376 Le Bourget-du-Lac Cedex, France
E-mail address: Denys.Dutykh@univ-savoie.fr
URL: http://www.lama.univ-savoie.fr/~dutykh/

IMA, University of Minnesota, 114 Lind Hall, 207 Church Street SE, Minneapolis MN 55455, USA
E-mail address: dmitsot@gmail.com
URL: http://sites.google.com/site/dmitsot/